ACCOUNTS of chemical research

Article

pubs.acs.org/accounts

Fe(II)-Polypyridines as Chromophores in Dye-Sensitized Solar Cells: A Computational Perspective

Published as part of the Accounts of Chemical Research special issue "Ultrafast Excited-State Processes in Inorganic Systems".

Elena Jakubikova* and David N. Bowman

Department of Chemistry, North Carolina State University, Raleigh, North Carolina 27695, United States

CONSPECTUS: Over the past two decades, dye-sensitized solar cells (DSSCs) have become a viable and relatively cheap alternative to conventional crystalline silicon-based systems. At the heart of a DSSC is a wide band gap semiconductor, typically a TiO_2 nanoparticle network, sensitized with a visible light absorbing chromophore. Ru(II)-polypyridines are often utilized as chromophores thanks to their chemical stability, long-lived metal-to-ligand charge transfer (MLCT) excited states, tunable redox potentials, and near perfect quantum efficiency of interfacial electron transfer (IET) into TiO_2. More recently, coordination compounds based on first row transition metals, such as Fe(II)-polypyridines, gained some attention as potential sensitizers in DSSCs due to their low cost and abundance. While such complexes can in principle sensitize TiO_2, they do so very inefficiently since their photoactive MLCT states undergo intersystem crossing (ISC) into low-lying metal-centered states on a subpicosecond time scale. Competition between the ultrafast ISC events and IET upon initial excitation of Fe(II)-polypyridines is the main obstacle to their utilization in DSSCs. Suitability of Fe(II)-polypyridines to serve as sensitizers could therefore be improved by adjusting relative rates of the ISC and IET processes, with the goal of making the IET more competitive with ISC.

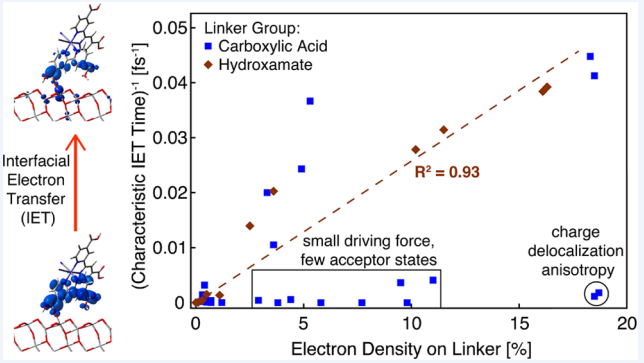

Our research program in computational inorganic chemistry utilizes a variety of tools based on density functional theory (DFT), time-dependent density functional theory (TD-DFT) and quantum dynamics to investigate structure−property relationships in Fe(II)-polypyridines, specifically focusing on their function as chromophores. One of the difficult problems is the accurate determination of energy differences between electronic states with various spin multiplicities (i.e., ^{1}A, ^{1,3}MLCT, ^{3}T, ^{5}T) in the ISC cascade. We have shown that DFT is capable of predicting the trends in the energy ordering of these electronic states in a set of structurally related complexes with the help of appropriate benchmarks, based either on experimental data or higher-level *ab initio* calculations.

Models based on TD-DFT and quantum dynamics approaches have proven very useful in understanding IET processes in Fe(II)-polypyridine−TiO_2 assemblies. For example, they helped us to elucidate the origin of "band selective" sensitization in the $[Fe(bpy\text{-}dca)_2(CN)_2]$−$TiO_2$ assembly (bpy-dca = 2,2′-bipyridine-4,4′-dicarboxylic acid), first observed by Ferrere and Gregg [Ferrere, S.; Gregg, B. A. *J. Am. Chem. Soc.* **1998**, *120*, 843.]. They also shed light on the relationship between the linker group that anchors Fe(II)-polypyridines onto the TiO_2 surface and the speed of IET in Fe(II)-polypyridine−TiO_2 assemblies.

More interestingly, our results show that the IET efficiency is strongly correlated with the amount of electron density on the linker group and that one can obtain insights into the IET in dye−semiconductor assemblies based on ground state electronic structure calculations alone. This may be useful for quick screening of a large number of complexes for use as potential sensitizers in DSSCs, especially if followed up by TD-DFT and quantum dynamics simulations for selected target compounds to confirm efficient sensitization. While our focus over the past few years has been exclusively on Fe(II)-polypyridines, the computational strategies outlined in this Account are applicable to a wide variety of sensitizers.

1. INTRODUCTION

The Sun is an abundant source of energy capable of meeting all our energy needs if properly harvested. However, efficient capture, storage, and transport of energy from sunlight still remain a challenge. Approaches to solar energy utilization include the conversion of sunlight to electricity via dye-sensitized solar cells (DSSCs)[1] or to chemical fuels via photocatalytic synthetic cells.[2] These systems are often designed around a single photoactive molecule (a chromophore) or a molecular array anchored to a semiconductor. The conversion of sunlight to electricity occurs via absorption of

Received: November 28, 2014
Published: April 28, 2015

DOI: 10.1021/ar500428t
Acc. Chem. Res. 2015, 48, 1441−1449

light by the chromophore, followed by the interfacial electron transfer (IET) between the chromophore and semiconductor.[3]

Some of the most efficient photocatalysts and photosensitizers are based on second or third row transition metals. For example, Ru(II)-polypyridines have attracted a large amount of attention as candidates for photoredox catalysts and sensitizers in solar cells.[4] They possess many properties that make them ideal for this task: chemical stability, long-lived ligand-centered excited-state lifetimes, and tunable redox potentials. In contrast, the photochemical activity of compounds based on first row transition metals is much more difficult to control, due to the presence of a number of low-lying metal-centered excited states of various spin multiplicities.[5] Their stability is also of concern.[6] At the same time, because of their low cost and abundance, coordination compounds based on first row transition metals lie at the heart of many efforts to develop more sustainable photovoltaic or artificial photosynthetic systems.[6−8]

Several first row transition metal complexes have been investigated as potential photosensitizers, among them coordination compounds of iron[9] and copper.[10] The first successful studies of Fe(II)-based compounds as sensitizers in DSSCs were performed by Ferrere and Gregg who showed that the $[Fe(bpy\text{-}dca)_2(CN)_2]$−$TiO_2$ system (bpy-dca = 2,2′-bipyridine-4,4′-dicarboxylic acid) undergoes band-selective IET from ultra-short-lived, initially excited, metal-to-ligand charge transfer (MLCT) states.[11] Later studies performed in the same laboratory investigated the effects of solvent and molecular anchoring groups on the photosensitization yields in these complexes.[9,12] Meyer et al. also studied the sensitization of nanocrystalline TiO_2 surfaces by $[Fe(bpy)(CN)_4]^{2-}$ complexes attached to TiO_2 via the CN^- ligands.[13] They observed sensitization phenomena in these systems, both via the direct excitation from the Fe d-orbitals into the Ti d-orbitals and by indirect sensitization via IET from the MLCT localized on the bpy ligand.

A common feature of all Fe(II)-polypyridine sensitized solar cells is their low efficiency in comparison with Ru(II)-polypyridine solar cells. This is due to the weaker ligand field (i.e, smaller t_{2g}−e_g gap) of iron complexes in comparison with the complexes of ruthenium. Therefore, in Fe(II)-polypyridines, metal-centered (MC) ligand-field states lie lower in energy than the lowest energy metal-to-ligand charge transfer state. As a result, initially excited ^{1}MLCT states of these complexes undergo an ultrafast intersystem crossing (ISC) into the lowest energy ^{5}MC states. Much work in elucidating the decay pathway from the initially excited ^{1}MLCT states has been done in the McCusker research group, who studied the ISC phenomenon in the tren-based polypyridine model complexes $[Fe(tren(py)_3)]^{2+}$ and $[Fe(tren(6\text{-}Me\text{-}py)_3)]^{2+}$.[5,7,14,15] The same process has been studied in some detail by Chergui and co-workers,[16] and more recently by Gaffney.[17]

Clearly, the competition between the ultrafast ISC event and IET upon the initial excitation of Fe(II)-polypyridines represents the main obstacle to their use as photosensitizers in the assemblies for solar energy conversion. Therefore, understanding various structural factors that influence the rates of the ISC and IET is important for rational design of more efficient Fe-based chromophores. Computational studies are especially well suited for such investigations because they allow one to evaluate the impact of systematic structural changes on various photophysical properties. In this Account, we summarize our computational efforts to employ density functional theory (DFT) and quantum dynamics simulations for systematic studies of ground and excited properties in these complexes.

2. CASE STUDIES

2.1. DFT as a Tool for Calculations of Fe(II)-Polypyridine Complexes

A prerequisite for successful computational studies of Fe(II)-polypyridine complexes is availability of computational methodologies capable of describing different properties, such as structure and absorption spectra. Fe-based compounds present a challenge for theoretical chemistry due to their relatively large size (∼50 or more atoms) and a number of energetically close lying states of various multiplicities. Because of their size, they are most amenable to DFT calculations. DFT has been proven to be an accurate tool for predicting the equilibrium geometries of these complexes,[18] as well as their absorption spectra using time-dependent DFT (TD-DFT) with hybrid functionals.[19] Obtaining the correct ground state, however, represents a major challenge for DFT since local functionals tend to favor the low-spin states, while the hybrid functionals favor high-spin states.[20] This behavior is directly related to the amount of exact Hartree−Fock (HF) exchange admixture used in the hybrid functionals (c_1).[21−23] The errors in the determination of the energy differences in high-spin and low-spin states ($\Delta E_{HS/LS}$) can be very large and the $\Delta E_{HS/LS}$ for a particular complex calculated by various DFT functionals can vary by as much as 80 kcal/mol (see Figure 1).

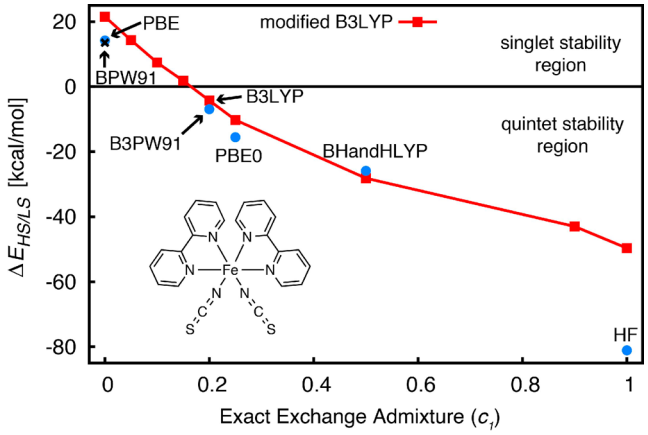

Figure 1. Calculated energy differences between singlet and quintet electronic states, $\Delta E_{HS/LS}$, for $[Fe(bpy)_2(NCS)_2]$ spin-crossover complex versus the fraction of exact exchange in the functional (c_1). Reproduced from ref 18. Copyright 2012 American Chemical Society.

There are at least two reasons why the ability to easily determine $\Delta E_{HS/LS}$ for Fe-based sensitizers is important. First, Fe(II)-polypyridines with singlet ground states absorb visible light with a greater intensity than complexes with the high-spin ground states.[15] Second, the ability to tune the ligand field strength of Fe(II)-polypyridines, and thus the energy ordering of various electronic states, may be important for slowing the rates of the ultrafast ISC events in these complexes.[24,25]

Reiher et al. suggested a reparametrization of B3LYP[26−29] resulting in the B3LYP* functional with reduced admixture of the HF exchange.[23] The B3LYP* functional has been successfully used in numerous studies on Fe(II) complexes.[22,24,30] Unfortunately, the admixture of the HF exchange

DOI: 10.1021/ar500428t
Acc. Chem. Res. 2015, 48, 1441−1449

in the hybrid functional strongly depends on the first row transition metal complex investigated, and it is difficult to know *a priori* the ideal value for this parameter.

While the exact determination of high-spin vs low-spin energy differences with DFT still remains a challenge, it is at least possible to qualitatively predict the effect of ligand substitutions on the spin transition behavior for a set of structurally related complexes.[31] But, how does one determine whether the complexes are structurally related to each other? We have recently demonstrated that structurally related complexes can be defined as pseudo-octahedral complexes that undergo similar distortion in the metal−ligand coordination environment between the high-spin and low-spin states.[18] Complexes with comparable average change in the metal−ligand bond lengths between the high- and low-spin structures (avg. $\Delta R_{HS/LS}$) display a very similar dependence of $\Delta E_{HS/LS}$ on the fraction of exact exchange admixture in the DFT functional (see Figure 2). This means that while the actual calculated high-

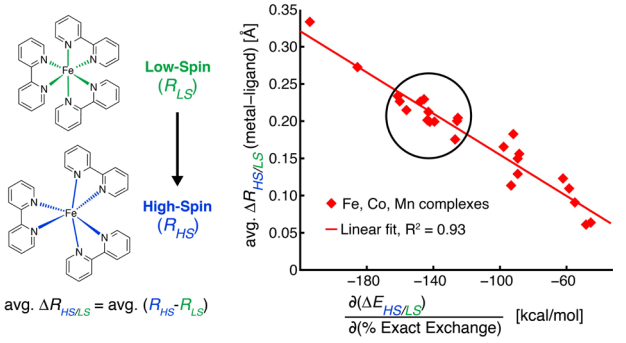

Figure 2. Average change in metal−ligand bond lengths ($\Delta R = R_{HS} - R_{LS}$) versus the change in $\Delta E_{HS/LS}$ with respect to exact exchange for a collection of Fe, Co, and Mn complexes. Reproduced from ref 18. Copyright 2012 American Chemical Society.

spin/low-spin energy differences vary substantially, relative energy ordering of the calculated $\Delta E_{HS/LS}$ in a series of structurally related complexes remains nearly constant across a range of exact exchange admixture in the DFT functional (see Figure 3). Therefore, one can determine the ground state of any octahedral first-row transition metal complex by comparison to a structurally related complex with known, exper-

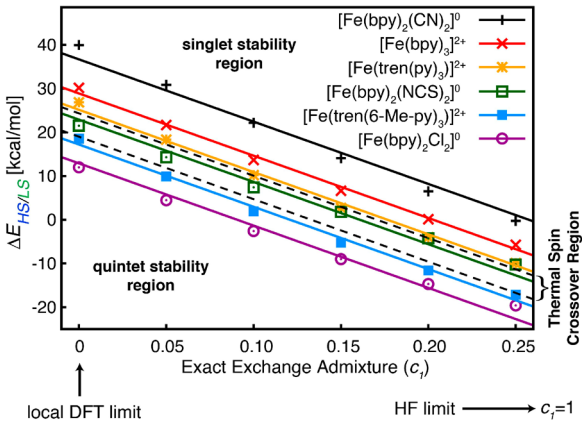

Figure 3. $\Delta E_{HS/LS}$ versus exact exchange in B3LYP functional for a set of structurally related complexes (circled in Figure 2). Reproduced from ref 18. Copyright 2012 American Chemical Society.

imentally determined ground state. This approach also enables one to obtain reliable trends in the energy differences of electronic states with different spin multiplicities, for example, when attempting to determine influence of structure on ligand field strength in a series of complexes.

An important point about utilizing the approach described in ref 18 is the need for a benchmark that can serve as a calibration point for comparison of the results obtained from DFT calculations. At minimum, one needs to know the electronic ground state for the benchmark complex; ideally $\Delta E_{HS/LS}$ or an experimental spin crossover temperature will be known as well. This benchmark can either be experimental (i.e., the set of structurally related complexes will include at least one with experimentally known ground state) or come from higher-level electronic structure calculations. At present, only CASPT2[30,32] or DMRG[33] approaches can reliably determine energy differences between the high-spin and low-spin states in the first row transition metal complexes. While these methodologies are computationally expensive, they are ideal for benchmarking purposes.[32,34] Since the relative energy ordering of the calculated $\Delta E_{HS/LS}$ in a series of structurally related complexes with respect to the benchmark (i.e., $\Delta E_{HS/LS}^{benchmark} - \Delta E_{HS/LS}$) remains nearly constant across a range of exact exchange admixture in the DFT functional (see Figure 3), any local or a hybrid DFT functional can be employed in the calculations. One simply needs to obtain the $\Delta E_{HS/LS}$ for the complexes of interest and compare them against the $\Delta E_{HS/LS}^{benchmark}$ of the benchmark complex. An example of a successful application of this approach to determination of ligand field strength for a series of cyclometalated Fe(II) complexes can be found in ref 35.

2.2. Band Selective Sensitization in Fe(II)-Polypyridine−TiO_2 Assemblies

An interesting aspect of Fe(II)-polypyridine chromophores is the unique way in which they sensitize TiO_2. This "band selective" sensitization behavior was first observed in $[Fe(bpy\text{-}dca)_2(CN)_2]$−$TiO_2$ assembly by Ferrere and Gregg, in which the $[Fe(bpy)_2(CN)_2]$ chromophore effectively sensitizes the TiO_2 semiconductor only from one of its two absorption bands in the visible region.[11] In contrast to this, the quantum yield for electron injection from the excited Ru(II)-polypyridine dyes into the TiO_2 conduction band is near unity, irrespective of their excitation wavelength.[36]

At the time of its discovery, the origin of the band selective sensitization phenomenon observed in $[Fe(bpy\text{-}dca)_2(CN)_2]$−$TiO_2$ was unknown. We have selected $[Fe(bpy\text{-}dca)_2(CN)_2]$−$TiO_2$ assembly as a starting point for our computational studies of iron-based sensitizers due to both the availability of experimental data in the literature and unanswered questions about its properties.[37,38] Our chosen computational protocol for studies of this and similar systems originates in the work of Batista and co-workers[39,40] and consists of the following steps: First, the absorption spectra of isolated dyes in solution are calculated by means of the DFT and TD-DFT approaches. Analysis of the calculated UV−vis absorption spectra provides us with the information on the character of the relevant excited states (metal centered, metal-to-ligand charge transfer, etc.) that serve as initial states for the IET between the excited dye and the semiconductor. Second, dye−TiO_2 nanoparticle models are created that are then employed in the quantum dynamics simulations of the IET. Since the dye−TiO_2 models contain over 900 atoms, extended Hückel (EH) rather than

DOI: 10.1021/ar500428t
Acc. Chem. Res. 2015, 48, 1441−1449

Kohn–Sham Hamiltonian is utilized in all quantum dynamics simulations. The initial wavepacket for the IET simulations is constructed by placing the excited electron into a virtual orbital on the dye (e.g., LUMO, LUMO+1) obtained from EH calculations that are matched to the relevant KS orbitals obtained from the DFT and TD-DFT calculations. In the case studies described here, the original Hoffmann Hückel parameter set was used in the EH calculations.[41,42] Note that if the EH calculations do not provide satisfactory match to the results obtained with DFT, reparametrization would be required. Finally, the rate of the IET in these systems is obtained via an exponential fit to the survival probability obtained in the course of the IET simulation, which describes the probability that the wavepacket is localized on the dye.

Several other methodologies are available for computational studies of IET in dye–TiO_2 assemblies. These include nonadiabatic molecular dynamics, real-time TD-DFT, Newns–Anderson type approaches, and nonequilibrium Green's function methods (see refs 43 and 44 and references therein). The approach employed in our work has been thoroughly tested for IET simulations in dye–TiO_2 assemblies.[39,40,45,46] Despite the simplifications, such as neglect of vibrational relaxation and electron–hole coupling, it is capable of describing short-term dynamics in a reliable manner.[47] Experimental evidence also suggests that IET in Fe(II)-polypyridine–TiO_2 assemblies occurs on a subpicosecond time scale, prior to vibrational relaxation.[7]

Figure 4 shows the absorption spectrum for the isolated $[Fe(bpy\text{-}dca)_2(CN)_2]$ in acetonitrile. In accordance with the experiment,[11] this dye displays two absorption bands in the visible region. Most of the excitations can be assigned as MLCT transitions. The excitations in the lower energy band, "Band 1", promote the electron into LUMO, LUMO+1, or a combination of the two orbitals, while the excitations in higher energy band, "Band 2", promote the electron into LUMO+2–LUMO+4 (MLCT transition) or to LUMO+12 (MC transitions). The initial wavepacket for the IET simulations in $[Fe(bpy\text{-}dca)_2(CN)_2]$–$TiO_2$ assemblies is thus created by placing an electron into one of these virtual orbitals. Nodal structures of LUMO–LUMO+4 and LUMO+12 orbitals obtained at both KS and EH level of theory are shown in Figure 4.

Example $[Fe(bpy\text{-}dca)_2(CN)_2]$–$TiO_2$ nanoparticle models used in the IET simulations are shown in Figure 5. In the case studies reported here, only the (101) surface of TiO_2 anatase was considered, because it is the most thermodynamically stable facet and phase of TiO_2 nanoparticles.[48] In general, it is necessary to consider multiple linker–nanoparticle surface binding modes. For carboxylic acid linker, previous computational and experimental studies suggest that both monodentate and bidentate binding modes are stable on the (101) TiO_2 anatase surface.[49,50] Additionally, there are two nonequivalent orientations of the $[Fe(bpy\text{-}dca)_2(CN)_2]$ dye on the TiO_2 surface, labeled as "bpy parallel" and "bpy perpendicular" based on the orientation of one of the bpy groups with respect to the surface (see Figure 5). Attachment of the chromophore via the nitrogen atom of the cyanide group was also considered for completeness, although experimental evidence suggests that $[Fe(bpy\text{-}dca)_2(CN)_2]$ preferentially binds to the TiO_2 surface through the carboxylic acid linker.[12]

Calculated characteristic IET times for various attachment modes of the $[Fe(bpy\text{-}dca)_2(CN)_2]$ on the (101) surface of TiO_2 anatase are shown in Figure 6. Comparison of the calculated IET characteristic times with the experimentally

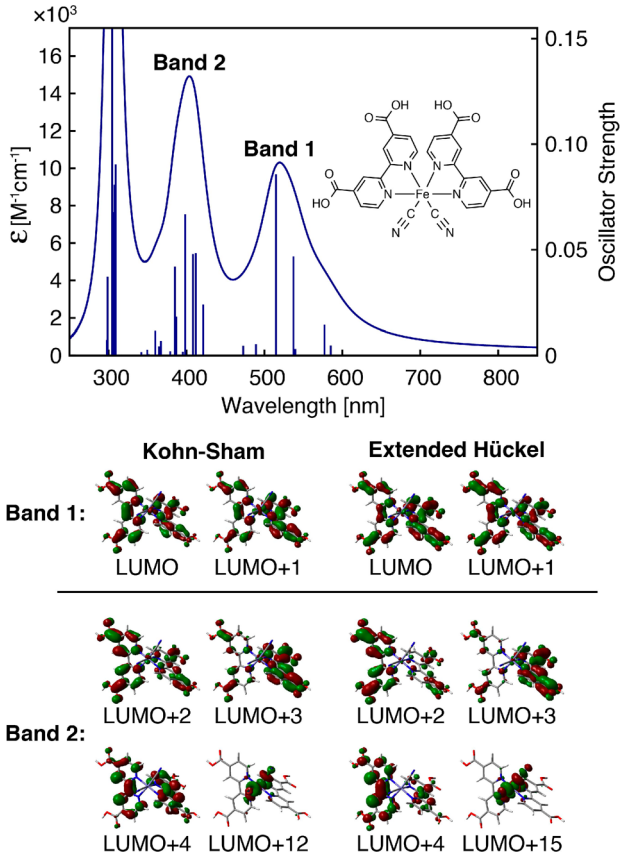

Figure 4. (top) Simulated absorption spectra for $[Fe(bpy\text{-}dca)_2(CN)_2]$ in acetonitrile (PCM) at the B3LYP level of theory. (bottom) Orbital contributions to particle states from Band 1 and 2 transitions (KS orbitals and matched EH orbitals). Reproduced from ref 37. Copyright 2013 American Chemical Society.

determined characteristic time for the ^{1}MLCT → ^{5}MC ISC process (~100 fs) suggests that IET from excited states originating in "Band 1" is not competitive with the ultrafast ISC process. On the other hand, several initial states populated by excitations in "Band 2" are capable of undergoing IET at the sub-100 fs time scale. One would, therefore, expect higher sensitization efficiency from the higher energy excitations (Band 2), and a significantly lower efficiency from the "Band 1" excitations, in accordance with the experimental studies of Ferrere and co-workers.[11]

The reason for the low efficiency is revealed by inspection of the density of states (DOS) in the energy region corresponding to the conduction band (CB) of the TiO_2 semiconductor. The initial states populated by the "Band 1" excitations, LUMO and LUMO+1, are located right at the edge of the TiO_2 CB, where a relatively small number of TiO_2 acceptor states are available. This reduces the efficiency of the IET to the point that it is no longer competitive with the ultrafast ISC in these complexes. The initial states populated by the "Band 2" excitations (LUMO+2–LUMO+4, LUMO+15) lie higher in the CB of TiO_2 with a significantly higher DOS of the semiconductor. These states also possess larger driving force for the IET than the states located at the CB edge, making them more competitive with the ultrafast ISC process. Therefore, one pathway toward the improvement of the Fe(II)-based sensitizers would be to raise the energies of LUMO and

DOI: 10.1021/ar500428t
Acc. Chem. Res. 2015, 48, 1441–1449

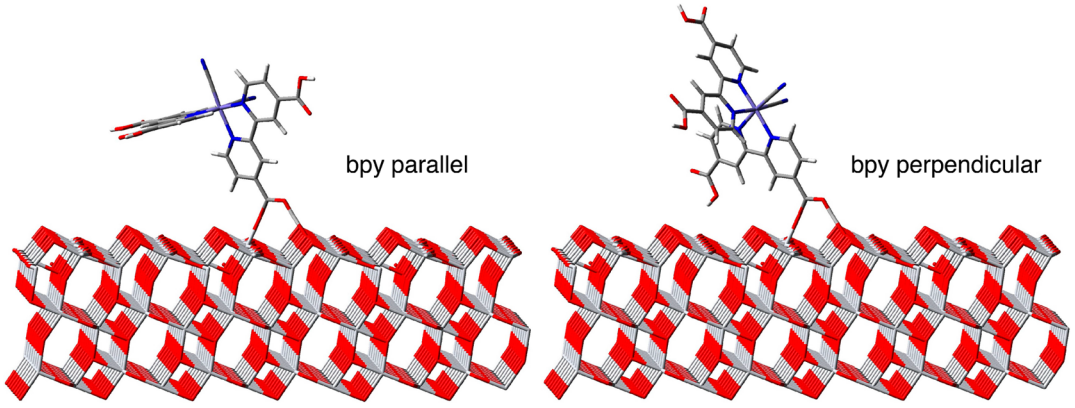

Figure 5. Example "bpy parallel" and "bpy perpendicular" orientations of $Fe(bpy\text{-}dca)_2(CN)_2$ on TiO_2. Reproduced from ref 37. Copyright 2013 American Chemical Society.

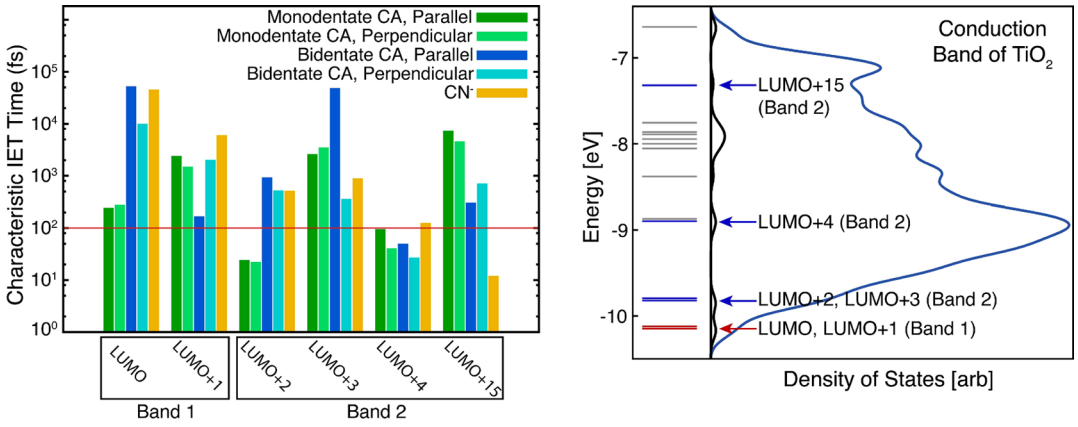

Figure 6. (left) Characteristic IET times for relevant particle states of $[Fe(bpy\text{-}dca)_2(CN)_2]$ attached to TiO_2. Red line at 100 fs represents characteristic ISC time for $^1MLCT \rightarrow {}^5MC$. (right) Energy levels of isolated $[Fe(bpy\text{-}dca)_2(CN)_2]$ chromophore and DOS (blue) and projected DOS (black) for the $[Fe(bpy\text{-}dca)_2(CN)_2]$–$TiO_2$ assembly calculated at the EH level of theory. Reproduced from refs 37 and 38. Copyright 2013 American Chemical Society.

LUMO+1 in order to improve their alignment with the CB of TiO_2.

2.3. Tuning IET in Dye–Semiconductor Assemblies

The competition between the ultrafast ISC process and IET in Fe(II)-polypyridine–TiO_2 assemblies is clearly the main reason for the poor performance of Fe(II)-polypyridines as sensitizers. Based on this, one can think of several ways to improve the efficiency of these Fe(II)-based sensitizers. These include speeding up the IET, slowing down the ISC, or completely eliminating the ISC in these systems. Various research groups have taken different approaches to this problem, mostly focusing on slowing down the ISC from the MLCT states by increasing the ligand field strength of Fe(II)-polypyridine complexes.[24,25,51,52] We have chosen to focus on finding ways to speed up the IET, so it becomes more competitive with the ISC process.[53]

A logical route to improving the rate of IET is by increasing the electronic coupling between the excited sensitizer donor states and the semiconductor acceptor states. Because the sensitizer is covalently bound to the surface of TiO_2 by a linker group, such as carboxylic acid, one would expect that the chemical structure of the linker would have a significant impact on the electronic coupling between the excited sensitizer and the semiconductor. Thus, we have chosen five different linker groups commonly used to attach various dyes to TiO_2[3,45,46] to investigate how they impact the IET rate in $[Fe(bpy\text{-}L)_2(CN)_2]$–$TiO_2$ assemblies (L = linker, see Figure 7).[53]

Our studies on a set of five different $[Fe(bpy\text{-}L)_2(CN)_2]$–$TiO_2$ assemblies utilized the computational protocol described

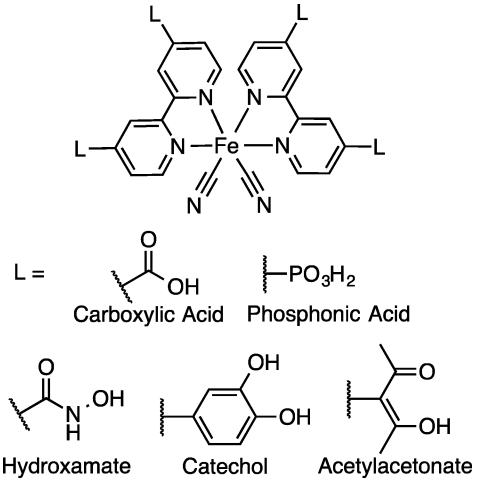

Figure 7. $[Fe(bpy)_2(CN)_2]$ functionalized with various linkers as shown. For catechol, the substitutions were performed independently at either the 4 or 4′ positions.

DOI: 10.1021/ar500428t
Acc. Chem. Res. 2015, 48, 1441–1449

in section 2.2. Additionally, we have developed a model for calculation of theoretical internal quantum efficiencies (TIQEs) in dye−semiconductor assemblies that combines the results of TD-DFT calculations with quantum dynamics simulations. Each transition at a particular wavelength of visible light (λ) is analyzed with the help of TD-DFT calculations in order to determine the composition of the particle states φ in terms of the virtual molecular orbitals ϕ_i:

$$\varphi = \sum_i c_i \phi_i$$

Based on this, survival probability at λ, $P(\lambda)$, is constructed as a linear combination of survival probabilities obtained from QD simulations utilizing the relevant initial states,

$$P(\lambda, t) = N \sum_i c_i^2 P(\phi_i, t), \qquad N = \frac{1}{\sum_i c_i^2}$$

where $P(\phi_i,t)$ is the survival probability obtained from the QD simulations utilizing ϕ_i as the initial wavepacket. The rate of the IET at a wavelength λ is then obtained as

$$k_{\mathrm{IET}}(\lambda) = \tau_{\mathrm{IET}}^{-1}(\lambda) = \left[\frac{\int_0^\infty tP(\lambda, t)\, \mathrm{d}t}{\int_0^\infty P(\lambda, t)\, \mathrm{d}t}\right]^{-1}$$

Finally, the TIQE at a particular wavelength λ is approximated as

$$\mathrm{TIQE}(\lambda) \propto \frac{k_{\mathrm{IET}}(\lambda)}{k_{\mathrm{IET}}(\lambda) + k_{\mathrm{ISC}}}$$

where the rate of the ISC, k_{ISC}, is set to $(100\ \mathrm{fs})^{-1}$ based on the experimental value determined for $[\mathrm{Fe(tren(py)_3)}]^{2+}$ and $[\mathrm{Fe(bpy)_3}]^{2+}$ complexes, closely related to $[\mathrm{Fe(bpy)_2(CN)_2}]$.[7,17] Since the identity of the linker group is not expected to significantly influence the ligand field strength of the complex, the ISC rate is assumed to be the same for all $[\mathrm{Fe(bpy\text{-}L)_2(CN)_2}]$ dyes investigated.

The calculation of theoretical internal quantum efficiency is highly desirable for two reasons: (1) it provides us with a direct comparison between the sensitization capabilities of different complexes and (2) internal quantum efficiency measurements are some of the most frequently utilized and published measures for judging the capabilities of constructed DSSC devices. Although our model provides only a simplistic view of dye−semiconductor assemblies (for example, it lacks explicit solvent and neglects the sensitizer−electrolyte or sensitizer−sensitizer interactions), we find that it is sufficient to describe qualitatively important features of Fe(II)-polypyridine sensitized TiO_2.

The calculated TIQEs at the discrete excitation energies for all $[\mathrm{Fe(bpy\text{-}L)_2(CN)_2}]$ dyes investigated are plotted along with their simulated absorption spectra in Figure 8. Based on these results, we can rank the linkers according to their capability to facilitate the IET transfer as follows: phosphonic acid < acetylacetonate < catechol < carboxylic acid < hydroxamate. Interestingly, our model predicts band-selective sensitization for all linkers investigated. Note that the $[\mathrm{Fe(bpy\text{-}L)_2(CN)_2}]$−$TiO_2$ assemblies with phosphonic and carboxylic acid linkers were prepared previously by Ferrere and co-workers.[9] In accordance with their results, our computational studies show greater IET efficiency in the $[\mathrm{Fe(bpy\text{-}dca)_2(CN)_2}]$−$TiO_2$ assemblies as well as the band-selective sensitization in assemblies containing both carboxylic and phosphonic acid linkers. More importantly, we suggest that hydroxamate and catechol linkers might serve as good alternatives to the more commonly used carboxylic acid linker.

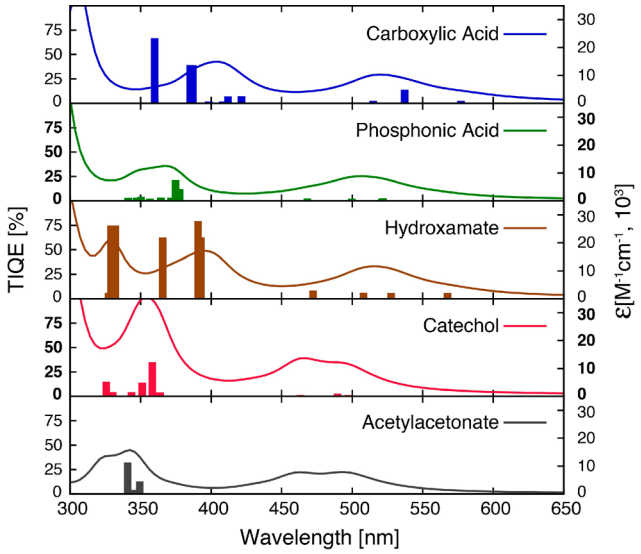

Figure 8. Idealized TIQEs (bars) for dye−TiO_2 assemblies with different linker groups, along with the absorption spectra (lines) of the molecular chromophores. τ_{ISC} was set to 100 fs. Reproduced from ref 53. Copyright 2015 IOP Publishing. Reproduced by permission of IOP Publishing. All rights reserved.

2.4. Criteria for Efficient IET in Fe(II)-Polypyridine−TiO_2 Assemblies

Computational studies described above elucidate the band-selective sensitization in Fe(II)-polypyridine−TiO_2 assemblies and suggest that the efficiency of the IET in these systems can be increased by a judicious choice of surface anchoring groups. Additionally, they provide us with more general insights into the IET processes in dye−nanoparticle assemblies, giving us a roadmap to rapid screening for efficient dyes using simple criteria, such as the percent of electron density on the linker.

There are three important conditions that influence the IET efficiency in dye−semiconductor assemblies in general: (1) driving force for the IET, which depends on the energy difference between the donor state of the dye and the edge of the CB of the semiconductor ($\Delta E_{\mathrm{D-CB}}$), (2) density of semiconductor acceptor states ($\rho_{\mathrm{accept.}}$), and (3) electronic coupling, or orbital overlap, between the donor states of the dye and the acceptor states of the semiconductor.[3,54,55] All three of these criteria have to be satisfied simultaneously in order to achieve IET with the characteristic time less than 100 fs. For example, all initially excited states in $[\mathrm{Fe(bpy)_2(CN)_2}]$−$TiO_2$ assemblies with the hydroxamate linker possess adequate driving force and are localized in the energy region with sufficient density of semiconductor states. Therefore, the rate of the IET in these systems is directly proportional (with a coefficient of determination of 0.93) to the orbital overlap between the initial dye-localized states and the semiconductor acceptor states, which is governed by the percent of electron density on the hydroxamate linker (see Figure 9).

The relationship between the percent of electron density on the linker and the rate of the IET is not as straightforward in case of the carboxylic acid linker. First, there are several states with approximately 3−11% of electron density on the linker

DOI: 10.1021/ar500428t
Acc. Chem. Res. 2015, 48, 1441−1449

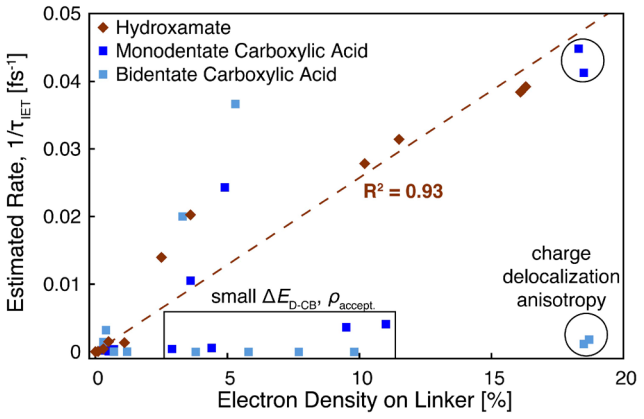

Figure 9. Reciprocal of characteristic IET time versus % of electron density on the linker for different donor states in $[Fe(bpy)_2(CN)_2]$–TiO_2 assemblies with carboxylic acid and hydroxamate linkers. The electron densities were calculated from Mulliken population analysis.[56] Boxed and circled points correspond to the LUMO/LUMO+1 and LUMO+2 of $[Fe(bpy\text{-}dca)_2(CN)_2]$, respectively.

that show much poorer IET rates than expected based on the electronic coupling alone (see states in a box in Figure 9). These states correspond to the LUMO and LUMO+1 of the $[Fe(bpy\text{-}dca)_2(CN)_2]$ complex that are not aligned well with the CB of TiO_2 (also see Figure 6).

The LUMO+2 initial state (shown in circles in Figure 9) is another interesting case. It is characterized by substantial electron density (~18–19%) on the carboxylic acid linker in both monodentate and bidentate attachment modes. The IET in $[Fe(bpy\text{-}dca)_2(CN)_2]$–$TiO_2$ assembly with a monodentate binding mode is, however, 1–2 orders of magnitude faster than in the assembly with a bidentate binding mode. Since the LUMO+2 donor states in both assemblies have almost same energy, the driving force and the density of acceptor states should be virtually identical for both. Inspection of the electron density over the course of simulation reveals that the differences between the IET rates are due to the differences in the speed of delocalization of the injected charge into the TiO_2 bulk. Anisotropy in the charge delocalization along different directions on the TiO_2 surface was observed in previous computational studies of dye–nanoparticle assemblies.[39]

Similar analysis can be done for all other dye–semiconductor assemblies with different linkers, yielding analogous results. Overall, the percent of electron density on the linker is a very strong predictor of the IET efficiency, but only if the other two criteria (adequate driving force and substantial density of acceptor states at the donor energy level) are satisfied as well. Information about the driving force and the density of acceptor states can be easily obtained from the DOS plots similar to that shown in Figure 6. The percent of electron density on the linker can be calculated from a population analysis. Therefore, qualitative insights into the IET in dye–semiconductor assemblies can be gained just by inspection of quantities easily acquired from the ground state electronic structure calculations, which should allow for quick screening of a large number of potential dyes and not only those based on Fe(II)-polypyridines. Note that this approach is more suited for screening out inefficient sensitizers than for the identification of ideal ones and should be followed by TD-DFT and IET studies of selected target compounds to confirm efficient sensitization.

3. SUMMARY

Over the past few years, we have established a computational strategy to investigate sensitization capabilities of Fe(II)-polypyridines employing DFT, TD-DFT, and quantum dynamics simulations.[18,35,37,38,53] Overall, DFT is a suitable tool for studies of Fe(II) complexes. Careful benchmarking of DFT against experimental data or higher-level *ab initio* calculations is necessary to obtain reliable information about the energy ordering of electronic states with different spin multiplicities.

Time-dependent DFT has also proved useful for calculations of excited state properties in Fe(II)-polypyridines. Along with the quantum dynamics simulations of the IET processes, it enabled us to explain band selective sensitization in $[Fe(bpy\text{-}dca)_2(CN)_2]$–$TiO_2$ assemblies and evaluate the impact of the sensitizer anchoring groups on the IET rates and internal quantum efficiencies.

Interestingly, insights into the IET in dye–semiconductor assemblies can be obtained from ground state electronic structure calculations alone. As is often the case with theoretical approaches, the trends obtained from the currently available computational models are more reliable than the actual calculated rates. Therefore, these models are utilized best as tools for systematic studies of a set of related complexes. The constant interplay between the theory and experiment is crucially important to further improve the current computational models and approaches. Finally, while our focus over the past few years has been exclusively on Fe(II)-polypyridines, the computational strategies outlined in this Account are applicable to a wide variety of sensitizers.

AUTHOR INFORMATION

Corresponding Author

*E-mail: ejakubi@ncsu.edu.

Notes

The authors declare no competing financial interest.

Biographies

Elena Jakubikova (Mgr. Physic, Comenius University; M.S. Mathematics and Ph.D. Chemistry, Colorado State University) is an Assistant Professor of Chemistry at North Carolina State University (NCSU).

David Bowman (B.S. Chemistry and Mathematics, Appalachian State University) is a Ph.D. candidate at NCSU.

ACKNOWLEDGMENTS

This research was supported by the Army Research Office Grant 59842-CH-II and North Carolina State University. D.N.B. also acknowledges support from the U.S. Department of Education GAANN Fellowship Program at NCSU.

REFERENCES

(1) Gratzel, M. Solar Energy Conversion by Dye-Sensitized Photovoltaic Cells. *Inorg. Chem.* **2005**, *44*, 6841–6851.
(2) Treadway, J. A.; Moss, J. A.; Meyer, T. J. Visible Region Photooxidation on TiO_2 with a Chromophore-Catalyst Molecular Assembly. *Inorg. Chem.* **1999**, *38*, 4386–4387.
(3) Hagfeldt, A.; Boschloo, G.; Sun, L.; Kloo, L.; Pettersson, H. Dye-Sensitized Solar Cells. *Chem. Rev.* **2010**, *110*, 6595–6663.
(4) Ardo, S.; Meyer, G. J. Photodriven Heterogeneous Charge Transfer with Transition-Metal Compounds Anchored to TiO_2 Semiconductor Surfaces. *Chem. Soc. Rev.* **2009**, *38*, 115–164.

DOI: 10.1021/ar500428t
Acc. Chem. Res. 2015, 48, 1441–1449

(5) Juban, E. A.; Smeigh, A. L.; Monat, J. E.; McCusker, J. K. Ultrafast Dynamics of Ligand-Field Excited States. *Coord. Chem. Rev.* **2006**, *250*, 1783−1791.
(6) Du, P.; Eisenberg, R. Catalysts Made of Earth-Abundant Elements (Co, Ni, Fe) for Water Splitting: Recent Progress and Future Challenges. *Energy Environ. Sci.* **2012**, *5*, 6012−6021.
(7) Monat, J. E.; McCusker, J. K. Femtosecond Excited-State Dynamics of an Iron(II) Polypyridyl Solar Cell Sensitizer Model. *J. Am. Chem. Soc.* **2000**, *122*, 4092−4097.
(8) Lu, X.; Wei, S.; Wu, C.-M. L.; Li, S.; Guo, W. Can Polypyridyl Cu(I)-Based Complexes Provide Promising Sensitizers for Dye-Sensitized Solar Cells? A Theoretical Insight into Cu(I) Versus Ru(II) Sensitizers. *J. Phys. Chem. C* **2011**, *115*, 3753−3761.
(9) Ferrere, S. New Photosensitizers Based Upon $[Fe^{II}(L)_2(CN)_2]$ and $[Fe^{II}L_3]$, Where L Is Substituted 2,2′-Bipyridine. *Inorg. Chim. Acta* **2002**, *329*, 79−92.
(10) Mara, M. W.; Fransted, K. A.; Chen, L. X. Interplays of Excited State Structures and Dynamics in Copper(I) Diimine Complexes: Implications and Perspectives. *Coord. Chem. Rev.* **2015**, *282*−*283*, 2−18.
(11) Ferrere, S.; Gregg, B. A. Photosensitization of TiO_2 by $[Fe^{II}(2,2'$-bipyridine-4,4′-dicarboxylic acid$)_2(CN)_2]$: Band Selective Electron Injection from Ultra-Short-Lived Excited States. *J. Am. Chem. Soc.* **1998**, *120*, 843−844.
(12) Ferrere, S. New Photosensitizers Based Upon $[Fe(L)_2(CN)_2]$ and $[Fe(L)_3]$ (L = Substituted 2,2′-Bipyridine): Yields for the Photosensitization of TiO_2 and Effects on the Band Selectivity. *Chem. Mater.* **2000**, *12*, 1083−1089.
(13) Yang, M.; Thompson, D. W.; Meyer, G. J. Dual Pathways for TiO_2 Sensitization by $Na_2[Fe(bpy)(CN)_4]$. *Inorg. Chem.* **2000**, *39*, 3738−3739.
(14) Huse, N.; Cho, H.; Hong, K.; Jamula, L.; de Groot, F. M. F.; Kim, T. K.; McCusker, J. K.; Schoenlein, R. W. Femtosecond Soft X-Ray Spectroscopy of Solvated Transition-Metal Complexes: Deciphering the Interplay of Electronic and Structural Dynamics. *J. Phys. Chem. Lett.* **2011**, *2*, 880−884.
(15) Smeigh, A. L.; Creelman, M.; Mathies, R. A.; McCusker, J. K. Femtosecond Time-Resolved Optical and Raman Spectroscopy of Photoinduced Spin Crossover: Temporal Resolution of Low-to-High Spin Optical Switching. *J. Am. Chem. Soc.* **2008**, *130*, 14105−14107.
(16) Bressler, C.; Milne, C.; Pham, V.-T.; ElNahhas, A.; van der Veen, R. M.; Gawelda, W.; Johnson, S.; Beaud, P.; Grolimund, D.; Kaiser, M.; Borca, C. N.; Ingold, G.; Abela, R.; Chergui, M. Femtosecond Xanes Study of the Light-Induced Spin Crossover Dynamics in an Iron(II) Complex. *Science* **2009**, *323*, 489−492.
(17) Zhang, W.; Alonso-Mori, R.; Bergmann, U.; Bressler, C.; Chollet, M.; Galler, A.; Gawelda, W.; Hadt, R. G.; Hartsock, R. W.; Kroll, T.; Kjaer, K. S.; Kubicek, K.; Lemke, H. T.; Liang, H. W.; Meyer, D. A.; Nielsen, M. M.; Purser, C.; Robinson, J. S.; Solomon, E. I.; Sun, Z.; Sokaras, D.; van Driel, T. B.; Vanko, G.; Weng, T. C.; Zhu, D.; Gaffney, K. J. Tracking Excited-State Charge and Spin Dynamics in Iron Coordination Complexes. *Nature* **2014**, *509*, 345−348.
(18) Bowman, D. N.; Jakubikova, E. Low-Spin Versus High-Spin Ground State in Pseudo-Octahedral Iron Complexes. *Inorg. Chem.* **2012**, *51*, 6011−6019.
(19) Laurent, A. D.; Jacquemin, D. TD-DFT Benchmarks: A Review. *Int. J. Quantum Chem.* **2013**, *113*, 2019−2039.
(20) Reiher, M. A Theoretical Challenge: Transition-Metal Compounds. *Chimia* **2009**, *63*, 140−145.
(21) Ganzenmüller, G.; Berkaïne, N.; Fouqueau, A.; Casida, M. E.; Reiher, M. Comparison of Density Functionals for Differences between the High- $(^5T_{2g})$ and Low- $(^1A_{1g})$ Spin States of Iron(II) Compounds. IV. Results for the Ferrous Complexes [Fe(L)('NHS4')]. *J. Chem. Phys.* **2005**, *122*, No. 234321.
(22) Reiher, M. Theoretical Study of the $Fe(phen)_2(NCS)_2$ Spin-Crossover Complex with Reparametrized Density Functionals. *Inorg. Chem.* **2002**, *41*, 6928−6935.
(23) Reiher, M.; Salomon, O.; Artur Hess, B. Reparameterization of Hybrid Functionals Based on Energy Differences of States of Different Multiplicity. *Theor. Chem. Acc.* **2001**, *107*, 48−55.
(24) Fredin, L. A.; Pápai, M.; Rozsályi, E.; Vankó, G.; Wärnmark, K.; Sundström, V.; Persson, P. Exceptional Excited-State Lifetime of an Iron(II)−N-Heterocyclic Carbene Complex Explained. *J. Phys. Chem. Lett.* **2014**, *5*, 2066−2071.
(25) Liu, Y.; Harlang, T.; Canton, S. E.; Chabera, P.; Suarez-Alcantara, K.; Fleckhaus, A.; Vithanage, D. A.; Goransson, E.; Corani, A.; Lomoth, R.; Sundstrom, V.; Warnmark, K. Towards Longer-Lived Metal-to-Ligand Charge Transfer States of Iron(II) Complexes: An N-Heterocyclic Carbene Approach. *Chem. Commun.* **2013**, *49*, 6412−6414.
(26) Becke, A. D. Density-Functional Thermochemistry. III. The Role of Exact Exchange. *J. Chem. Phys.* **1993**, *98*, 5648−5652.
(27) Lee, C.; Yang, W.; Parr, R. G. Development of the Colle-Salvetti Correlation-Energy Formula into a Functional of the Electron Density. *Phys. Rev. B* **1988**, *37*, 785−789.
(28) Becke, A. D. Density-Functional Exchange-Energy Approximation with Correct Asymptotic Behavior. *Phys. Rev. A* **1988**, *38*, 3098−3100.
(29) Stephens, P. J.; Devlin, F. J.; Chabalowski, C. F.; Frisch, M. J. Ab Initio Calculation of Vibrational Absorption and Circular Dichroism Spectra Using Density Functional Force Fields. *J. Phys. Chem.* **1994**, *98*, 11623−11627.
(30) Pápai, M.; Vankó, G.; de Graaf, C.; Rozgonyi, T. Theoretical Investigation of the Electronic Structure of Fe(II) Complexes at Spin-State Transitions. *J. Chem. Theory Comput.* **2013**, *9*, 509−519.
(31) Paulsen, H.; Duelund, L.; Zimmermann, A.; Averseng, F.; Gerdan, M.; Winkler, H.; Toftlund, H.; Trautwein, A. X. Substituent Effects on the Spin-Transition Temperature in Complexes with Tris(pyrazolyl) Ligands. *Monatsh. Chem.* **2003**, *134*, 295−306.
(32) Pierloot, K.; Vancoillie, S. Relative Energy of the High-$(^5T_{2g})$ and Low-$(^1A_{1g})$ Spin States of the Ferrous Complexes [Fe(L)-(NHS4)]: CASPT2 Versus Density Functional Theory. *J. Chem. Phys.* **2008**, *128*, No. 034104.
(33) Reiher, M. A Theoretical Challenge: Transition-Metal Compounds. *Chimia* **2009**, *63*, 140−145.
(34) Swart, M. Accurate Spin-State Energies for Iron Complexes. *J. Chem. Theory Comput.* **2008**, *4*, 2057−2066.
(35) Mukherjee, S.; Bowman, D. N.; Jakubikova, E. Cyclometalated Fe(II) Complexes as Sensitizers in Dye-Sensitized Solar Cells. *Inorg. Chem.* **2015**, *54*, 560−569.
(36) Hamann, T. W.; Jensen, R. A.; Martinson, A. B.; Van Ryswyk, H.; Hupp, J. T. Advancing Beyond Current Generation Dye-Sensitized Solar Cells. *Energy Environ. Sci.* **2008**, *1*, 66−78.
(37) Bowman, D. N.; Blew, J. H.; Tsuchiya, T.; Jakubikova, E. Elucidating Band-Selective Sensitization in Iron(II) Polypyridine-TiO_2 Assemblies. *Inorg. Chem.* **2013**, *52*, 8621−8628.
(38) Bowman, D. N.; Blew, J. H.; Tsuchiya, T.; Jakubikova, E. Correction to Elucidating Band-Selective Sensitization in Iron(II) Polypyridine-TiO_2 Assemblies. *Inorg. Chem.* **2013**, *52*, 14449.
(39) Rego, L. G. C.; Batista, V. S. Quantum Dynamics Simulations of Interfacial Electron Transfer in Sensitized TiO_2 Semiconductors. *J. Am. Chem. Soc.* **2003**, *125*, 7989−7997.
(40) Jakubikova, E.; Snoeberger, R. C., III; Batista, V. S.; Martin, R. L.; Batista, E. R. Interfacial Electron Transfer in TiO_2 Surfaces Sensitized with Ru(II)−Polypyridine Complexes. *J. Phys. Chem. A* **2009**, *113*, 12532−12540.
(41) Summerville, R. H.; Hoffmann, R. Tetrahedral and Other M_2L_6 Transition Metal Dimers. *J. Am. Chem. Soc.* **1976**, *98*, 7240−7254.
(42) Hoffmann, R. An Extended Hückel Theory. I. Hydrocarbons. *J. Chem. Phys.* **1963**, *39*, 1397−1412.
(43) Martsinovich, N.; Troisi, A. Theoretical Studies of Dye-Sensitised Solar Cells: From Electronic Structure to Elementary Processes. *Energy Environ. Sci.* **2011**, *4*, 4473−4495.
(44) Akimov, A. V.; Neukirch, A. J.; Prezhdo, O. V. Theoretical Insights into Photoinduced Charge Transfer and Catalysis at Oxide Interfaces. *Chem. Rev.* **2013**, *113*, 4496−4565.

DOI: 10.1021/ar500428t
Acc. Chem. Res. 2015, 48, 1441−1449

(45) McNamara, W. R.; Snoeberger, R. C., III; Li, G. H.; Richter, C.; Allen, L. J.; Milot, R. L.; Schmuttenmaer, C. A.; Crabtree, R. H.; Brudvig, G. W.; Batista, V. S. Hydroxamate Anchors for Water-Stable Attachment to TiO_2 Nanoparticles. *Energy Environ. Sci.* **2009**, *2*, 1173−1175.
(46) McNamara, W. R.; Snoeberger, R. C., III; Li, G.; Schleicher, J. M.; Cady, C. W.; Poyatos, M.; Schmuttenmaer, C. A.; Crabtree, R. H.; Brudvig, G. W.; Batista, V. S. Acetylacetonate Anchors for Robust Functionalization of TiO_2 Nanoparticles with Mn(II)-Terpyridine Complexes. *J. Am. Chem. Soc.* **2008**, *130*, 14329−14338.
(47) Hoff, D. A.; da Silva, R.; Rego, L. G. C. Coupled Electron−Hole Quantum Dynamics on D−π−A Dye-Sensitized TiO_2 Semiconductors. *J. Phys. Chem. C* **2012**, *116*, 21169−21178.
(48) Zhang, H.; Banfield, J. L. Thermodynamic Analysis of Phase Stability of Nanocrystal Titania. *J. Mater. Chem.* **1998**, *8*, 2073−2076.
(49) Leon, C. P.; Kador, L.; Peng, B.; Thelakkat, M. Characterization of the Adsorption of Ru-bpy Dyes on Mesoporous TiO_2 Films with UV-vis, Raman, and FTIR Spectroscopies. *J. Phys. Chem. B* **2006**, *110*, 8723−8730.
(50) Vittadini, A.; Selloni, A.; Rotzinger, F. P.; Gratzel, M. Formic Acid Adsorption on Dry and Hydrated TiO_2 Anatase (101) Surfaces by DFT Calculations. *J. Phys. Chem. B* **2000**, *104*, 1300−1306.
(51) Jamula, L. L.; Brown, A. M.; Guo, D.; McCusker, J. K. Synthesis and Characterization of a High-Symmetry Ferrous Polypyridyl Complex: Approaching the $^5T_2/^3T_1$ Crossing Point for Fe(II). *Inorg. Chem.* **2014**, *53*, 15−17.
(52) Dixon, I. M.; Khan, S.; Alary, F.; Boggio-Pasqua, M.; Heully, J. L. Probing the Photophysical Capability of Mono and Bis-(cyclometallated) Fe(II) Polypyridine Complexes Using Inexpensive Ground State DFT. *Dalton Trans.* **2014**, *43*, 15898−15905.
(53) Bowman, D. N.; Mukherjee, S.; Barnes, L. J.; Jakubikova, E. Linker Dependence of Interfacial Electron Transfer Rates in Fe(II)−Polypyridine Sensitized Solar Cells. *J. Phys.: Condens. Matter* **2015**, *27*, No. 134205.
(54) Anderson, N. A.; Lian, T. Ultrafast Electron Transfer at the Molecule-Semiconductor Nanoparticle Interface. *Annu. Rev. Phys. Chem.* **2005**, *56*, 491−519.
(55) She, C.; Guo, J.; Irle, S.; Morokuma, K.; Mohler, D. L.; Zabri, H.; Odobel, F.; Youm, K.-T.; Liu, F.; Hupp, J. T.; Lian, T. Comparison of Interfacial Electron Transfer through Carboxylate and Phosphonate Anchoring Groups. *J. Phys. Chem. A* **2007**, *111*, 6832−6842.
(56) Mulliken, R. S. Electronic Population Analysis on LCAO−MO Molecular Wave Functions. I. *J. Chem. Phys.* **1955**, *23*, 1833−1840.

DOI: 10.1021/ar500428t
Acc. Chem. Res. 2015, 48, 1441−1449